0026-895X/05/6802-457–466$20.00
MOLECULAR PHARMACOLOGY
Copyright © 2005 The American Society for Pharmacology and Experimental Therapeutics
Mol Pharmacol 68:457–466, 2005

Vol. 68, No. 2
11270/3043388
Printed in U.S.A.

Single Nucleotide Polymorphisms in the Human Norepinephrine Transporter Gene Affect Expression, Trafficking, Antidepressant Interaction, and Protein Kinase C Regulation

Maureen K. Hahn, Michelle S. Mazei-Robison, and Randy D. Blakely

Department of Pharmacology (M.K.H., M.S.M.-R., R.D.B.) and Center for Molecular Neuroscience (M.K.H., R.D.B.), Vanderbilt University School of Medicine, Nashville, Tennessee

Received January 20, 2005; accepted May 11, 2005

ABSTRACT

The role of norepinephrine (NE) in attention, memory, affect, stress, heart rate, and blood pressure implicates NE in psychiatric and cardiovascular disease. The norepinephrine transporter (NET) mediates reuptake of released catecholamines, thus playing a role in the limitation of signaling strength in the central and peripheral nervous systems. Nonsynonymous single nucleotide polymorphisms (SNPs) in the human NET (*hNET*) gene that influence transporter function can contribute to disease, such as the nonfunctional transporter, A457P, identified in orthostatic intolerance. Here, we examine additional amino acid variants that have been identified but not characterized in populations that include cardiovascular phenotypes. Variant hNETs were expressed in COS-7 cells and were assayed for protein expression and trafficking using cell-surface biotinylation and Western blot analysis, transport of radiolabeled substrate, antagonist interaction, and regulation through protein kinase C (PKC)-linked pathways by the phorbol ester β-phorbol-12-myristate-13-acetate. We observed functional perturbations in 6 of the 10 mutants studied. Several variants were defective in trafficking and transport, with the most dramatic effect observed for A369P, which was completely devoid of the fully glycosylated form of transporter protein, was retained intracellularly, and lacked any transport activity. Furthermore, A369P and another trafficking variant, N292T, impeded surface expression of hNET when coexpressed. F528C demonstrated increased transport and, remarkably, exhibited both insensitivity to down-regulation by PKC and a decrease in potency for the tricyclic antidepressant desipramine. These findings reveal functional deficits that are likely to compromise NE signaling in SNP carriers in the population and identify key regions of NET contributing to transporter biosynthesis, activity, and regulation.

Norepinephrine (NE) released at central and peripheral synapses is inactivated through active transport into terminals by the presynaptically localized norepinephrine transporter (NET) (Iversen, 1961). NET recaptures as much as 90% of released NE in the heart, making it a critical mediator of NE inactivation and presynaptic catecholamine homeostasis (Schomig et al., 1989). Indeed, NET knockout mice exhibit a diminished rate of extracellular NE clearance in the brain, elevated extracellular NE concentrations in brain and plasma, reduced tissue NE concentrations in brain and heart, and altered dopamine (DA) signaling in brain (Xu et al., 2000; Keller et al., 2004). NET is also a target for tricyclic antidepressants, NET-selective reuptake inhibitors, and psychostimulants, including cocaine, methylphenidate, and amphetamine (Fuller and Hemrick-Luecke, 1983; Tatsumi et al., 1997). The human NET (*hNET*) gene is a single-copy gene (SLC6A2) located on chromosome 16 containing 16 exons (Hahn and Blakely, 2002b). hNET is a member of the SLC6A family of Na^+/Cl^--dependent transporters with a predicted protein topology of 12 transmembrane domains with intracellularly localized NH_2 and COOH termini (Pacholczyk et al., 1991; Hahn and Blakely, 2002a). A large extracellular loop contains 3 *N*-glycosylation sites (Melikian et al., 1996).

This work was supported by National Institutes of Health grants HL56693 and MH58921 (to R.D.B.) and F32-MH12896 (to M.K.H.).
Article, publication date, and citation information can be found at http://molpharm.aspetjournals.org.
doi:10.1124/mol.105.011270.

ABBREVIATIONS: NE, norepinephrine; NET, norepinephrine transporter; h, human; SNP, single nucleotide polymorphism; PKC, protein kinase C; KRH, Krebs-Ringer-HEPES; BIM, bisindolylmaleimide I; β-PMA, phorbol-12-myristate-13-acetate; RIPA, radioimmunoprecipitation; OCT1, organic cation transporter 1; TM, transmembrane domain; SERT, serotonin transporter; DAT, dopamine transporter; ADHD, attention-deficit/hyperactivity disorder; DA, dopamine; HA, hemagglutinin; PBS, phosphate-buffered saline; PBS/Ca/Mg, phosphate-buffered saline containing $CaCl_2$ and $MgCl_2$; HRP, horseradish peroxidase; ANOVA, analysis of variance.

NET transport activity can be regulated by multiple signal-transduction mechanisms, such as protein kinase C (PKC) (Apparsundaram et al., 1998).

The importance of NET to NE homeostasis suggests a role for NET in disorders of both the central and autonomic nervous systems. Involvement of noradrenergic systems in mood disorders is suggested by evidence that depression is accompanied by altered indices of noradrenergic function and that effective antidepressants enhance extracellular NE levels (Ressler and Nemeroff, 1999). Furthermore, NET binding sites are decreased in the brains of patients with major depression (Klimek et al., 1997). The activation and sensitization of NE systems in response to stress suggest that NE may play a role in disorders triggered by early life trauma, including depression and post-traumatic stress disorder (Heim and Nemeroff, 2001). NE also plays an important role in attention, vigilance, learning, and memory and is hypothesized to contribute to attention-deficit/hyperactivity disorder (ADHD) (Biederman and Spencer, 1999). Stimulant drugs used to treat ADHD act on both the NET and the DA transporter (DAT), and atomoxetine, which selectively targets NET, is also effective in treating ADHD (Biederman and Spencer, 1999). The activity of NET at postganglionic sympathetic nerve terminals, especially in the heart, is impacted in diseases of the cardiovascular system (Blakely, 2001; Hahn and Blakely, 2002a). Diminished NE uptake sites and activity have been observed in hypertension, diabetes, cardiomyopathy, and heart failure, and ischemia-induced efflux of nonvesicular, cytoplasmic NE via NET may also contribute to fatal arrhythmias (Hahn and Blakely, 2002a).

The importance of NET in the homeostasis of NE in brain and autonomic nervous system, evidence of its dysfunction in disease, and its role as a target for therapeutics raise the question of whether alterations in NE homeostasis or drug response derive from hNET genetic variation. A number of *hNET* promoter, intron, and coding-region polymorphisms have been identified either through discovery-oriented studies of *hNET* in various clinical populations or during the course of genome sequencing efforts (Hahn and Blakely, 2002a). To date, approximately 20 nonsynonymous single nucleotide polymorphisms (SNPs), which result in amino acid substitutions, have been reported in *hNET*. Many of these variants were derived from psychiatric and cardiovascular phenotypes, yet only a limited number have been examined for alterations in expression or function (Stöber et al., 1996; Halushka et al., 1999; Runkel et al., 2000; Iwasa et al., 2001). Our laboratory identified, in a familial form of orthostatic intolerance, a nonsynonymous *hNET* SNP that produces the protein variant, A457P, which is a loss-of-function, dominant-negative transporter that contributes to increased heart rate and plasma norepinephrine levels (Shannon et al., 2000; Hahn et al., 2003). Overall, these findings suggest that cardiovascular phenotypes could be enriched for *hNET* SNPs that produce functional alterations. In the present work, we examine the functional impact of amino acid variants primarily found in cardiovascular phenotypes. We observe changes in protein expression levels, including aberrant processing by glycosylation and altered surface expression, with variants exhibiting abolished or greatly diminished plasma membrane expression. Furthermore, coexpression of hNET with variants exhibiting greatly altered processing generates a dominant-negative impact on hNET expression and cell-surface targeting. We demonstrate changes in both NE and DA transport that reveal effects of variants on substrate selectivity. Finally, in a single variant, F528C, we observe both a shift in the potency of the tricyclic antidepressant desipramine and a novel regulatory phenotype of resistance to regulation through PKC-mediated pathways.

Materials and Methods

Plasmid Constructs. The expression vector pcDNA3 (Invitrogen, Carlsbad, CA) containing the coding sequence for hNET, pcDNA3-hNET, bearing an introduced AflII site was used in the construction of the *hNET* nonsynonymous SNPs, R121Q, V244I, N292T, V356L, A369P, N375S, K463R, F528C, Y548H, and I549T. Single-point mutations were generated using the QuikChange Site-Directed Mutagenesis Kit (Stratagene, La Jolla, CA) according to the manufacturer's instructions. A BglII site was created at position 436 (accession no. NM_001043) to facilitate subcloning. Sequences were confirmed using dideoxynucleotide terminators (Center for Molecular Neuroscience Neurogenomics Core, Vanderbilt University, Nashville, TN). In some experiments, an HA epitope-tagged hNET construct was used to distinguish hNET from cotransfected hNET variants.

Cell Culture and Transfection. All experiments were performed in transiently transfected COS-7 cells (American Type Culture Collection, Manassas, VA). COS-7 cells were maintained in Dulbecco's modified Eagle's medium (Invitrogen) supplemented with 10% fetal bovine serum (HyClone Laboratories, Logan, UT), L-Glutamine (2 mM) (Invitrogen), and 100 U/ml penicillin/100 μg/ml streptomycin (Invitrogen) in a humidified incubator at 37°C and 5% CO_2. One day before transfection, cells were plated in individual wells of 24-well plates at a density of 5×10^4 cells/well. Transfection was performed using FuGene 6 reagent as described by the manufacturer (Roche Applied Science, Indianapolis, IN). All experimental manipulations were begun ~24 h after transfection. Observations in all experiments were made using multiple DNA stocks to control for any variability in DNA plasmid preparation.

[^{3}H]NE Transport Assays. Transport was assayed essentially as described previously (Hahn et al., 2003). In brief, cells were washed twice with Krebs-Ringer-HEPES buffer (KRH; 120 mM NaCl, 4.7 mM KCl, 1.2 mM KH_2PO4, 2.2 mM $CaCl_2$, and 10 mM HEPES, pH 7.4) and preincubated with assay buffer (KRH, 10 mM D-glucose, 100 μM ascorbic acid, 100 μM pargyline, and 1 mM tropolone) for 10 min at 37°C, with 1 μM desipramine added to a subset of wells to assess nonspecific accumulation, followed by the addition of radiolabeled substrate for a 10-min transport assay. In experiments using a single concentration of substrate, 50 nM concentrations of [^{3}H]NE or [^{3}H]DA (~36 or ~49 Ci/mmol, respectively; Amersham Biosciences AB, Uppsala, Sweden) were used. Saturation kinetics to determine K_m and V_{max} values were carried out using serial dilutions of NE or DA (100 nM to 10 μM) with [^{3}H]NE or [^{3}H]DA of constant specific activity, respectively. In experiments assessing the effects of drugs on transport, drugs were added before the addition of [^{3}H]NE, and this preincubation time varied. In experiments of phorbol ester regulation of NET, cells were incubated in 1 μM bisindolylmaleimide I (BIM; Calbiochem, San Diego, CA) or 1 μM staurosporine (Sigma-Aldrich, St. Louis, MO) for 20 min, followed by the addition of 100 nM phorbol-12-myristate-13-acetate (β-PMA; Sigma-Aldrich) for 5, 10, or 30 min before the addition of [^{3}H]NE. In some experiments, cells were treated with 100 nM or 1 μM β-PMA for 30 min before the addition of [^{3}H]NE. In experiments to determine the inhibition of [^{3}H]NE uptake by antagonists, cells were incubated for 10 min at 37°C with cocaine or desipramine (both from Sigma-Aldrich) followed by the addition of [^{3}H]NE to a final concentration of 50 nM for 10 min of uptake at 37°C. After uptake, cells were washed three times in KRH, incubated for 2 h in Microscint 20 scintillation fluid (PerkinElmer Life and Analytical Sciences, Boston, MA), and accu-

mulated radiolabeled substrate was quantified in a Topcount plate scintillation counter (PerkinElmer).

K_m and V_{max} values were calculated by nonlinear regression analysis according to a single-site hyperbolic model (Prism version 4; GraphPad Software Inc., San Diego, CA). K_i values for the inhibition of [^{3}H]NE uptake by antagonists were calculated for data expressed as the percentage inhibition of total uptake versus the log of drug concentration by nonlinear regression analysis according to a single-site competition model (Prism software).

Cell-Surface Biotinylation and Immunoblots. To investigate the effect of hNET SNPs on protein expression and trafficking, cell-surface biotinylation was performed on intact cells (Hahn et al., 2003). Cells were washed four times in 1× PBS and were incubated with 1.0 mg/ml sulfosuccinimidyl 2-(biotinamido)-ethyl-1, 3-dithiopropionate (Pierce Chemical, Rockford, IL) in PBS containing 0.1 mM $CaCl_2$ and 1.0 mM $MgCl_2$ (PBS/Ca/Mg) for 20 min at 4°C, washed, quenched with three washes of 100 mM glycine in PBS/Ca/Mg, and washed two times in PBS/Ca/Mg. Cells were lysed in radioimmunoprecipitation (RIPA) buffer (10 mM Tris, pH 7.4, 150 mM NaCl, 1 mM EDTA, 0.1% SDS, 1% Triton X-100, 1% sodium deoxycholate, 250 μM phenylmethylsulfonyl fluoride, 1 μg/ml aprotinin, 1 μg/ml leupeptin, and 1 μM pepstatin) for 30 min at 4°C, centrifuged at 20,000*g* for 30 min, and supernatants were assayed for protein concentration using a BCA kit (Pierce). Equal amounts of protein were incubated with Immunopure Immobilized Streptavidin beads (Pierce) for 45 min at room temperature. Beads were washed four times in RIPA buffer, and proteins bound to beads were eluted in 1× sample buffer (62.5 mM Tris, pH 6.8, 20% glycerol, 2% SDS, 5% β-mercaptoethanol, and 0.01% bromphenol blue). Samples were then separated by 10% SDS-polyacrylamide gel electrophoresis. Proteins were transferred electrophoretically to Immobilon-P membrane (Millipore Corporation, Billerica, MA). Membranes were incubated with a monoclonal antibody directed against hNET at a dilution of 1:500 (NET17-1; Mab Technologies, Inc., Stone Mountain, GA) followed by incubation with a goat anti-mouse peroxidase-conjugated secondary antibody at a dilution of 1:5000 (Jackson ImmunoResearch Laboratories Inc., West Grove, PA). In cotransfection experiments that used an HA-tagged hNET, an HRP-conjugated anti-HA antibody was used at a dilution of 1:500 (Roche Applied Science). Visualization of immunoreactivity was achieved using Western Lightning Enhanced Chemiluminescent Reagent (PerkinElmer).

Quantification of Immunoblots. Quantification of band density was performed on scanned images using ImageJ, a public domain image-processing program (W. Rasband, National Institute of Mental Health, Bethesda, MD). The optical density of each lane was plotted, and the area under the curve was measured for both the 110- and the 54-kDa NET immunoreactive bands. Analyses were performed on replicate experiments, and data are presented both in graph form of the means ± S.E.M. of repeated experiments and with blots of a representative experiment.

Statistical Analysis. Data were analyzed using one-way analysis of variance (ANOVA) with levels of significance set at $p < 0.05$ (SPSS for Windows, release 7.0; SPSS Inc., Chicago, IL). The contribution of individual group means to overall significant F values was determined by Fisher's least-square difference post hoc test, with $p < 0.05$ considered significant.

Results

Multiple naturally occurring variants have been identified in *hNET*, although only a few have been functionally assessed (Fig. 1) (Halushka et al., 1999; Runkel et al., 2000; Shannon et al., 2000; Iwasa et al., 2001; Hahn et al., 2003). In the present work, we examined a group of these uncharacterized SNPs, most of which were detected in populations with cardiovascular phenotypes. (Fig. 1, ○; Table 1). Seven of these SNPs encoding the amino acid changes N292T, V356L, A369P, N375S, K463R, F528C, and Y548H were identified in a study of both African-Americans and Americans with Northern European ancestry with blood pressure measures in the upper and lower 2.5th percentile using high-density microarray chips (Halushka et al., 1999). R121Q was found in a study of Japanese patients with long QT syndrome and was identified in both the control and long QT groups (Iwasa et al., 2001). I549T has been observed by several groups in populations of Asian and European ancestry and is deposited at dbSNP, the SNP database at the National Center for Biotechnology and Informatics. These SNPs have been validated by observance of the minor allele in more than one chromosome and/or by multiple independent submissions, and Table 1 lists their estimated frequencies (dbSNP; Halushka et al., 1999; Iwasa et al., 2001). Our laboratory, using denaturing high-performance liquid chromatography followed by dideoxy sequencing confirmation, identified V244I in one individual with no defined phenotype. These SNPs occur at amino acids with extremely high conservation among NETs of various species as well as among NETs, DATs, and serotonin transporters (SERTs) (Table 2). The variants occur throughout the transporter in both transmembrane domains (TMs) and loop regions (Fig. 1). Site-directed mutagenesis was used to generate these SNPs in the hNET cDNA in the expression vector pcDNA3.

All assays were performed 24 h after transfection of the hNET cDNA (hereafter termed hNET) or variant hNETs at equal DNA concentrations into COS-7 cells. To assess the influence of hNET SNPs on transporter expression, total and cell-surface protein was measured using a cell-impermeant biotinylating reagent followed by immunoblotting of Streptavidin-recovered protein. Previous work from our lab demonstrates that steady-state profiles of hNET from heterologous expression systems comprise several different species of protein arising from different stages of progression through the biosynthetic pathway (Melikian et al., 1994; Hahn et al., 2003). In transiently transfected COS-7 cells, the major forms observed are 46, 54, and 80 to 110 (termed 110 here-

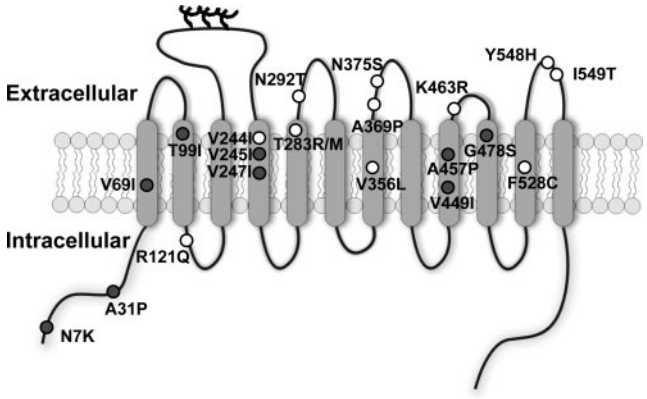

Fig. 1. Schematic representation of hNET depicting the amino acid variants generated by nonsynonymous SNPs that have been identified (Stöber et al., 1996; Halushka et al., 1999; Shannon et al., 2000; Iwasa et al., 2001; dbSNP). hNET is depicted as a 12-transmembrane domain-spanning protein with intracellular NH_2- and COOH-termini. For the variants shown, the number refers to the amino acid position in the protein and is preceded by the single-letter code for the amino acid commonly at that position followed by the single letter code for the variant. The approximate positions of the variant residues are indicated by ○ and ●. The variants represented by ○ are those evaluated in the present report.

after) kDa that represent, respectively, unglycosylated, core-glycosylated, and highly glycosylated forms of the transporter, with the 110-kDa form preferentially expressed on the plasma membrane (Hahn et al., 2003). Analysis of hNET variants revealed several distinct protein expression profiles (Figs. 2 and 3). Evaluation of the 54- and 110-kDa forms of NET in total and surface pools revealed mutant-dependent changes in protein expression levels suggestive of alterations in both glycosylation and trafficking (total 54-kDa form, $F_{10,41} = 21.25$, $p < 0.001$; surface 54-kDa form, $F_{10,36} = 10.47$, $p < 0.001$; total 110-kDa form, $F_{10,40} = 7.64$, $p < 0.001$; surface 110-kDa form, $F_{10,42} = 10.53$, $p < 0.001$). A369P expressed the 54-kDa form of hNET at levels comparable with that of hNET, whereas the 110-kDa form was essentially absent in total lysates and in the biotinylated fraction (Figs. 2, A and B, and 3, A and B). F528C demonstrated a 22% increase in total lysate levels of the 110-kDa protein and a 35%, increase in 110-kDa surface levels (Figs. 2, A and B, and 3, A and B). Total and surface levels of the 110-kDa form of R121Q were 83.8 ± 4.1 and 72.1 ± 5.9% of hNET, respectively, with surface levels significantly different from those of hNET (Figs. 2, A and B, and 3, A and B). Y548H expressed surface levels of the 110-kDa form that were 71.7 ± 10.6% of hNET, a decrease that did not reach significance (Figs. 2B and 3B). N292T shows an aberrant glycosylation pattern in which a large amount of protein remains in the nonglycosylated 46-kDa form and other forms of varying size are present, including the 54- and 110-kDa forms, creating a smeared appearance on blots (Fig. 2A). The 110-kDa form of N292T in total lysate was 20.0 ± 12.9% of hNET, although this value is difficult to estimate because of the continuous nature of the distribution of N292T protein. It is striking that the biotinylated fraction reveals that much of the anomolous N292T remains intracellular, whereas the 110- and 54-kDa forms are expressed on the surface, as is the nonglycosylated 46-kDa form (Fig. 2B). The surface levels of the 110-kDa form are decreased to levels 50.7 ± 13.7% of hNET, whereas there was a large increase in the surface expression of the 54-kDa form (Figs. 2B and 3B). Finally, there was a significant decrease in I549T protein in surface fractions that was not evident in the totals (Figs. 2 and 3).

Transport assays of 50 nM [^{3}H]NE or [^{3}H]DA were next performed to determine the functional capacity of all hNET variants. Several SNPs altered the transport of [^{3}H]NE ($F_{10,32} = 23.61$, $p < 0.001$) or [^{3}H]DA ($F_{10,32} = 19.26$, $p < 0.001$) (Fig. 4 and Table 3). A369P failed to transport either [^{3}H]NE or [^{3}H]DA (Fig. 4). N292T exhibited decreased transport of [^{3}H]NE and [^{3}H]DA (62.2 ± 4.8 and 67.7 ± 6.6% of hNET, respectively), whereas Y548H demonstrated a more modest reduction of transport of [^{3}H]NE and [^{3}H]DA (77.7 ± 6.3 and 79.7 ± 6.9% of hNET, respectively) (Fig. 4). Cells expressing F528C yielded an increase in [^{3}H]NE transport to 131.0 ± 11.1% of hNET, whereas [^{3}H]DA transport was unchanged for this variant. R121Q transport rates of [^{3}H]NE and [^{3}H]DA were decreased to 56 and 72% of hNET, respectively. Comparison of the ratios of [^{3}H]NE with [^{3}H]DA transport among transporter variants revealed significant changes in substrate selectivity ($F_{10,32} = 2.64$, $p < 0.05$) (Table 3). As noted, F528C demonstrated an increased transport of [^{3}H]NE versus [^{3}H]DA compared with hNET. Al-

TABLE 2

Sequence alignment among NETs, DATs, and SERT for hNET variant amino acid positions

	Amino Acid Position in hNET									
	121	244	292	356	369	375	463	528	548	549
hNET	R	V	N	V	A	N	K	F	Y	I
macaqueNET	R	V	N	V	A	N	K	F	Y	I
mNET	R	V	N	I	A	N	K	F	Y	T
RNET	R	V	N	I	A	K	K	F	Y	V
bNET	R	V	N	I	A	N	K	F	Y	I
gallusNET	R	V	N	I	A	K	N	F	Y	T
quailNET	R	V	N	I	A	K	N	F	Y	T
FET	R	V	S	I	A	K	N	F	Y	N
hDAT	R	V	R	S	A	P	N	F	Y	I
macaqueDAT	R	V	R	S	A	P	N	F	Y	I
mDAT	R	V	R	S	A	P	N	F	Y	I
rDAT	R	V	R	S	A	P	N	F	Y	I
bDAT	R	V	R	S	A	P	N	F	Y	V
zebrafishDAT	R	V	K	F	S	A	N	F	Y	Y
cEDAT	R	V	E	L	S	P	E	I	Y	T
mothDAT	R	V	Q	V	A	D	K	F	Y	V
hSERT	R	I	L	V	A	D	F	F	Y	N
macaqueSERT	R	I	L	V	A	D	F	F	Y	N
mSERT	R	I	V	V	A	D	S	F	Y	N
rSERT	R	I	V	V	A	D	S	F	Y	N
ovineSERT	R	I	L	V	A	D	F	F	Y	D
caviaSERT	R	I	L	V	A	D	F	F	Y	S
bSERT	R	I	L	V	A	D	F	F	Y	D
gallusSERT	R	I	L	V	A	D	F	F	Y	N
dSERT	R	V	K	L	A	S	Y	F	Y	Y
cESERT	R	V	Y	F	S	P	Y	F	Y	T
manducaSERT	R	V	R	L	A	S	Y	F	Y	T

m, mouse; r, rat; b, bovine; f, frog; h, human; cE, *Caenorhabditis elegans*; d, *Drosophila melanogaster*; ET, epinephrine transporter.

TABLE 1

Nonsynonymous single nucleotide polymorphisms in *hNET* gene

Subset of identified hNET variants evaluated in the present study. Nucleotide positions are from GenBank accession numbers X91117 to X91127. Exon and intron numbers reflect the revised structure of the hNET gene following identification of a new exon 1 (Kim et al., 1999).

Gene Position	Nucleotide	Protein Position	Amino Acid Variant			Frequency	Reference
			Major	Position	Minor		
Exon 3	G299A	IL1	Arg	121	Gln	G = 0.995, A = 0.005	Iwasa et al., 2001
Exon 5	G223A	TM4	Val	244	Ile	G = 0.99, A = 0.01	Blakely Lab
Exon 6	A258C	EL3	Asn	292	Thr	A = 0.90, C = 0.10	Halushka et al., 1999
Exon 8	G193C	TM7	Val	356	Leu	G = 0.90, C = 0.10	Halushka et al., 1999
Exon 8	G232C	EL4	Ala	369	Pro	G = 0.95, C = 0.05	Halushka et al., 1999
Exon 8	A251G	EL4	Asn	375	Ser	A = 0.90, G = 0.10	Halushka et al., 1999
Exon 10	A256G	EL5	Lys	463	Arg	A = 0.90, G = 0.10	Halushka et al., 1999
Exon 12	T233G	TM11	Phe	528	Cys	T = 0.90, G = 0.10	Halushka et al., 1999
Exon 13	T776C	EL6	Tyr	548	His	T = 0.90, G = 0.10	Halushka et al., 1999
Exon 13	T780C	EL6	Ile	549	Thr	T = 0.99, C = 0.03	dbSNP

IL, intracellular loop; EL, extracellular loop; TM, transmembrane domain (as predicted by Pacholczyk et al., 1991).

though the change in the ratio of R121Q [^{3}H]NE to [^{3}H]DA transport did not reach significance in the single-point assay, significant differences were observed in R121Q substrate transport when saturation kinetics were determined (see below).

Saturation kinetics for both [^{3}H]NE and [^{3}H]DA transport were obtained for variants that demonstrated altered transport in the single-point assays. Because of its complete lack of surface expression and transport, A369P was not included in these assays. Cells expressing R121Q, N292T, F528C, or Y548H all demonstrated altered kinetic profiles compared with hNET (NE: $F_{4,14} = 18.50$, $p < 0.001$; DA: $F_{4,14} = 28.15$, $p < 0.001$). We also examined the ratios of V_{max} to K_m values as measures of transporter efficiency and found that ratios significantly changed for several mutants (NE: $F_{4,14} = 93.5$, $p < 0.01$; DA: $F_{4,14} = 5.11$; $p < 0.05$). First, similar to findings in the single-point assays, F528C demonstrated an increased V_{max} for [^{3}H]NE transport (Fig. 5A). The F528C K_m value for NE, although consistently somewhat lower, was not significantly different from that for hNET. DA V_{max} was also elevated (Fig. 5B). The V_{max}-to-K_m ratio of F528C transport of [^{3}H]NE was twice that of hNET (6.1 ± 0.3 versus 3.1 ± 0.2, respectively), whereas the V_{max}-to-K_m ratio for [^{3}H]DA was not significantly elevated. Saturation kinetics of R121Q revealed a significant decrease in V_{max} for [^{3}H]NE transport to 65.6 ± 1.4% of hNET. In contrast, the V_{max} for [^{3}H]DA transport decreased only to 91.0 ± 8.1% of hNET (Fig. 5, A and B). The R121Q V_{max}-to-K_m ratio was decreased to half that of hNET using [^{3}H]NE as the substrate (1.4 ± 0.3 versus 3.1 ± 0.2, respectively) but remained unchanged with respect to [^{3}H]DA. This was contributed to by a consistent, although not significant, increase in the R121Q K_m value for NE. N292T was diminished in both [^{3}H]NE and [^{3}H]DA transport, with V_{max} values of 43.5 ± 6.3 and 48.1 ± 5.6% of hNET, respectively (Fig. 5, A and B). Y548H NE and DA

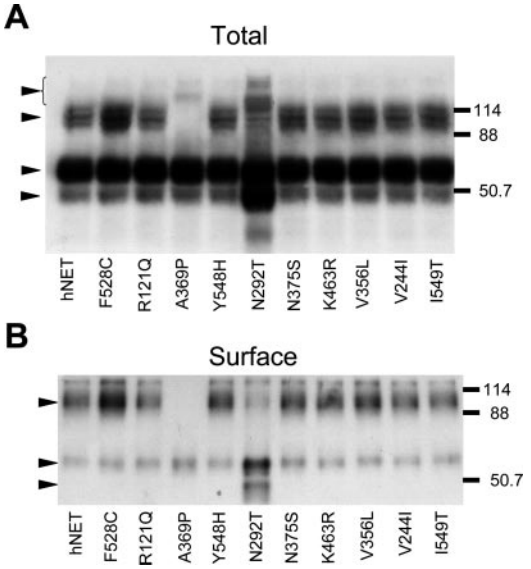

Fig. 2. Western blot analysis of hNET and variant total cellular lysate (A) and surface expression (B). COS-7 cells were transfected with hNET or variant cDNAs as described under *Materials and Methods*. Twenty-four hours later, cells were incubated in sulfosulfosuccinimidyl 2-(biotinamido)-ethyl-1, 3-dithiopropionate followed by extraction in RIPA buffer containing protease inhibitors. Aliquots containing equal amounts of protein were taken from each sample for total hNET, and from the remaining sample, aliquots of equal amounts of protein were extracted with streptavidin beads as described under *Materials and Methods*. Blots were probed with a monoclonal antibody to hNET (NET-17-1) followed by a goat anti-mouse HRP-conjugated secondary antibody and chemiluminescent detection. Arrows indicate different molecular mass forms of hNET described in the text. Molecular masses indicated are from prestained standards run in parallel and are noted in kilodaltons.

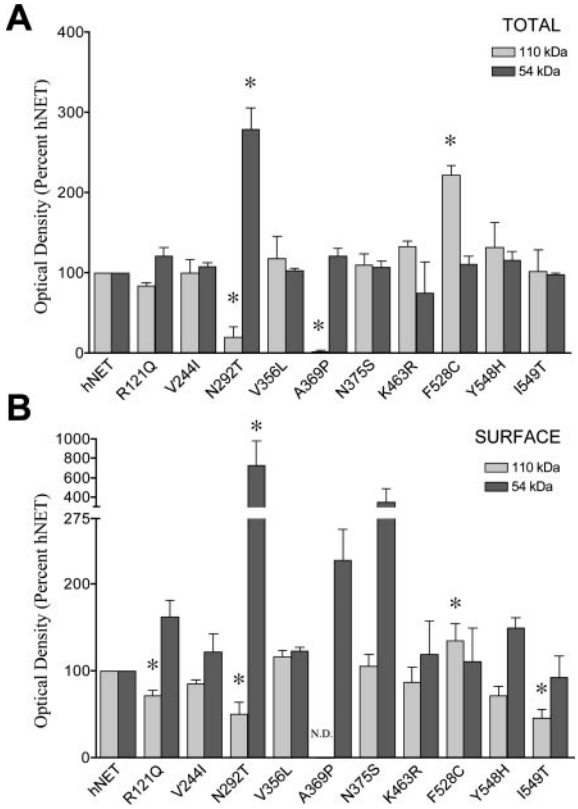

Fig. 3. Quantification of hNET and variant protein expression in total cellular lysate (A) and surface fractions (B) in transiently transfected COS-7 cells described in Fig. 2. Optical density was measured for each band with ImageJ software as described under *Materials and Methods*. Results are expressed as a percentage of hNET band density for each protein species and are the mean ± S.E.M. of three experiments. Data were analyzed by one-way ANOVA as described under *Materials and Methods*; *, $p < 0.05$.

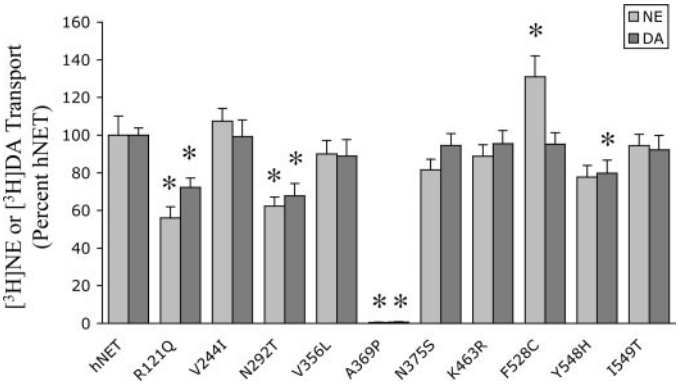

Fig. 4. [^{3}H]NE and [^{3}H]DA transport of hNET and variants. COS-7 cells were transiently transfected with hNET or variant cDNAs. Twenty-four hours later, radiolabeled uptake was performed as described under *Materials and Methods* using 50 nM [^{3}H]NE (light gray bars) or 50 nM [^{3}H]DA (dark gray bars). Nonspecific uptake was defined by 1 μM desipramine. hNET transport of [^{3}H]NE and [^{3}H]DA was 6.3 ± 0.6 × 10^{-18} and 1.1 ± 0.04 × 10^{-17} mol/cell/min, respectively). Data are expressed as the percentage [^{3}H]NE or [^{3}H]DA uptake of hNET. Data are the mean ± S.E.M. of three experiments and were analyzed by one-way ANOVA as described under *Materials and Methods*. *, $p < 0.05$.

V_{max} values were 87.8 ± 5.4 and 82.2 ± 3.2% of hNET, respectively, changes that reached significance for the decrease in DA transport (Fig. 5, A and B).

We also tested the effect of hNET variants on the ability of transporter inhibitors to compete for [^{3}H]NE transport, targeting cocaine and desipramine as a prototypical psychostimulant and tricyclic antidepressant, respectively. In general, only modest shifts in K_i values were observed. One exception was F528C, which demonstrated a significant increase in the K_i value for desipramine competition of NE uptake, losing potency by approximately 8-fold (4.7 ± 0.6 versus 40.9 ± 6.0 nM; $F_{9,30} = 24.50$; $p < 0.001$).

The changes in F528C and R121Q expression levels coupled with substrate-specific transport properties suggested that in addition to trafficking alterations, there might be compromised regulation by signal-transduction mechanisms. A well-studied mechanism of hNET regulation is the PKC-mediated down-regulation that occurs in response to receptor stimulation or direct activation of PKC with phorbol esters (Apparsundaram et al., 1998). We therefore tested the ability of the phorbol ester β-PMA to down-regulate R121Q and F528C compared with hNET. Thirty minutes of 100 nM or 1 μM β-PMA decreased [^{3}H]NE uptake by approximately 40% (Fig. 6A). Treatment with either 100 nM or 1 μM β-PMA for 30 min resulted in a significantly greater decrease in transport by R121Q compared with hNET, whereas F528C was unaffected by β-PMA treatment (Fig. 6A). Incubation with 100 nM β-PMA for 10 min in the presence or absence of PKC inhibitors was performed to examine the specificity of these effects. Ten-minute β-PMA treatment resulted in a 25% decrease in hNET [^{3}H]NE transport that was completely blocked by 1 μM staurosporine or 1 μM BIM (Fig. 6B) ($F_{5,17} = 9.88$, $p < 0.001$). R121Q again demonstrated a greater decrease in [^{3}H]NE transport compared with hNET in response to 10 min of β-PMA treatment ($p < 0.05$; Fig. 6B). The effect on R121Q was also completely blocked by staurosporine or BIM ($F_{5,17} = 6.38$, $p < 0.01$). F528C was completely resistant to the effects of 10-min treatment with 100 nM β-PMA ($F_{5,17} = 1.23$; Fig. 6B). There was a trend for PKC inhibitors to increase basal levels of transport for hNET and R121Q, an effect that was significant for the staurosporine-induced increase in uptake for hNET (Fig. 6B). This suggests the presence of tonic regulation of hNET in COS-7 cells that can be relieved by staurosporine. It is interesting to note that F528C showed no such effect of PKC inhibitors on basal transport, again indicating the insensitivity of F528C to regulation by PKC-linked pathways.

The heterozygous nature of hNET SNPs coupled with evidence of oligomer formation by neurotransmitter transporters compelled us to examine the influence of coexpression of hNET variants on hNET. Variants that exhibited altered processing and trafficking of transporter protein, R121Q, F528C, N292T, and A369P, were each cotransfected with an equal amount of HA-tagged hNET followed by cell-surface biotinylation and Western blot analysis. Both N292T and A369P exhibited marked effects on hNET expression when cotransfected (total 54-kDa form: $F_{4,14} = 5.61$, $p < 0.05$; surface 54-kDa form, $F_{4,14} = 16.58$, $p < 0.001$; surface 110-kDa form: $F_{4,14} = 12.05$, $p < 0.001$; total 110-kDa $F_{4,13} = 10.39$, $p < 0.01$). N292T produced a dramatic decrease in total hNET expression of both 54- and 110-kDa forms and greatly diminished surface expression (Fig. 7, A–D). A369P also diminished total and surface expression of hNET (Fig. 7, A–D). [^{3}H]NE transport for all hNET and variant coexpressed conditions was intermediate to transport levels of hNET or the variant expressed alone (data not shown). We also measured the effect of β-PMA in cotransfection experiments to test the ability of variants to confer functional changes to a presumed transporter complex. Cotransfection of R121Q or F528C with hNET followed by 30-min treatment with 1 μM β-PMA resulted in regulation that was intermediate between the effects of β-PMA on hNET or either variant expressed singly (data not shown). Likewise, cotransfection of R121Q and F528C, which individually produce the most divergent phenotypes, with respect to β-PMA regulation, also generated a β-PMA response intermediate to that observed in cells transfected with either variant alone (data not shown).

To evaluate a potential correlation of functional effects with amino acid substitution of each variant, we examined the BLOSUM62 scores of the *hNET* SNPs. The BLOSUM62 is a scoring matrix that infers protein function for amino acid substitutions (Henikoff and Henikoff, 1992). In a study that examined gene mutations in the organic cation transporter OCT1, Leabman and coworkers (2003) predicted that substitutions at residues conserved in all members of mammalian OCT1 orthologs would be more deleterious than those at evolutionarily unconserved residues (Leabman et al., 2003).

TABLE 3

Transport and surface expression of hNET SNPs in COS-7 cells

Data are the mean ± S.E.M. of three experiments. Transport and surface expression of protein are expressed as a percentage of wild type for each measure. Data were analyzed using one-way ANOVA followed by Fisher's least-squares difference.

hNET Variant	Transport		Transport Ratio of [^{3}H]NE/[^{3}H]DA	Surface Expression (110-kDa form)
	[^{3}H]NE	[^{3}H]DA		
	50 nM, % hNET			
R121Q	56.0 ± 5.9*	72.2 ± 5.1*	0.78 ± 0.11	72.1 ± 5.8*
V244I	107.4 ± 6.6	99.2 ± 8.8	1.10 ± 0.10	85.1 ± 4.8
N292T	62.3 ± 4.8*	67.7 ± 6.6*	0.93 ± 0.09	50.7 ± 13.7*
V356L	90.0 ± 7.1	88.9 ± 8.7	1.02 ± 0.08	116.5 ± 7.9
A369P	0.5 ± 0.2*	0.7 ± 0.2*	0.77 ± 0.38	N.D.
N375S	81.5 ± 5.7	94.6 ± 6.2	0.87 ± 0.08	105.2 ± 13.8
K463R	88.8 ± 6.0	95.4 ± 6.9	0.93 ± 0.05	87.6 ± 16.9
F528C	131.0 ± 11.1*	95.2 ± 6.1	1.39 ± 0.15*	134.7 ± 20.6*
Y548H	77.7 ± 6.3*	79.7 ± 6.9*	0.99 ± 0.11	71.7 ± 10.6
I549T	94.4 ± 6.1	92.1 ± 7.7	1.03 ± 0.06	46.1 ± 9.6*

* $p < 0.05$.
N.D., not detectable.

The majority of OCT1 mutations at conserved residues decreased function, whereas none of the unconserved changes affected function. Furthermore, the BLOSUM62 scores were more negative (evolutionarily unfavorable) for the variants that decreased function, and most with non-negative scores exhibited normal function. When the *hNET* SNPs evaluated in the present study were divided into two groups: one with those found to exert effects on protein expression, substrate transport, inhibitor binding, or regulation by PKC (R121Q, A369P, N292T, F528C, Y548H, and I549T), and a second having no effect on these measures (V244I, V356L, N375S, and K463R); the group of variants conferring functional changes had significantly lower BLOSUM62 scores (-1.14 ± 0.28) than those deemed to have no effects on function (1.75 ± 0.48) ($p < 0.05$; Student's two-tailed t test).

Discussion

Although it is likely that complex disorders result from multiple gene and environmental influences, candidate gene approaches remain attractive when a strong argument can be advanced for the role of a gene in disease, particularly when endophenotypes are examined. We identified previously a nonfunctional, dominant-negative hNET mutation that contributes to a phenotype of orthostatic intolerance, tachycardia, and elevated plasma NE levels (Shannon et al., 2000; Hahn et al., 2003). Most of the SNPs in the present study were identified in extreme blood pressure or long QT syndrome (Halushka et al., 1999; Iwasa et al., 2001). The present results reveal striking effects of these naturally occurring SNPs on transporter protein expression, substrate transport, antagonist interaction, and regulation by kinase-mediated signaling pathways. The use of selective phenotypes should continue to reveal hNET variants with functional consequences that, although they may be limited to a small number of cases or families, could greatly contribute to phenotypes in those individuals.

Among the hNET variants evaluated in the present study, V244I, V356L, N375S, and K463R had little effect on hNET expression levels or transport of NE and DA and could represent variation retained in the population because of a lack

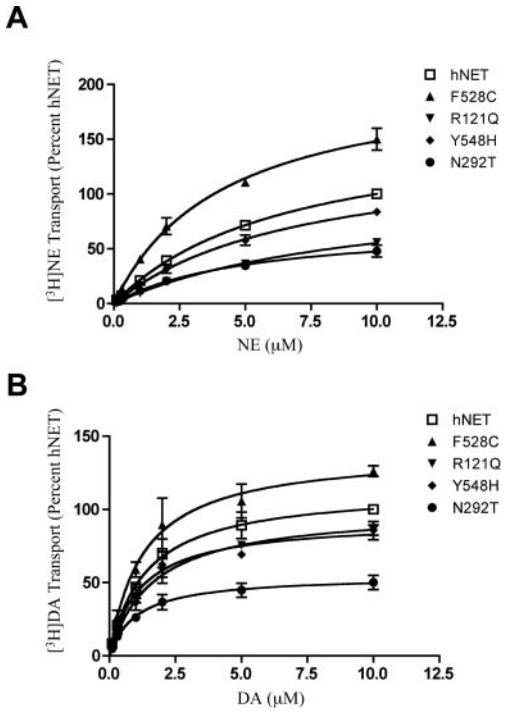

Fig. 5. Saturation kinetics of [^{3}H]NE (A) and [^{3}H]DA (B) uptake of hNET and variant hNETs. COS-7 cells were transiently transfected with hNET or variant cDNAs. Twenty-four hours later, saturation transport assays were performed as described under *Materials and Methods*. Transport was determined by incubating cells for 10 min with 100 nM to 10 μM [^{3}H]NE or [^{3}H]DA, and nonspecific activity was defined by 1 μM desipramine at each concentration. Data are expressed as the percentage of hNET transport at 10 μM concentration of substrate and are the mean ± S.E.M. values of three experiments. K_m and V_{max} values were determined using Prism as described under *Materials and Methods*. Data were analyzed using one-way ANOVA followed by Fisher's least-square difference test; *, $p < 0.05$. NE transport V_{max} (moles × 10^{-16}/cell/min) and K_m (in micromoles) values, respectively, were as follows: hNET, 2.1 ± 0.3 and 6.8 ± 1.3; R121Q, 1.4 ± 0.2 and 9.8 ± 2.4; N292T, 0.9 ± 0.02 and 5.2 ± 0.7; F528C, 2.6 ± 0.2 and 4.2 ± 0.7; Y548H, 1.8 ± 0.3 and 7.4 ± 0.8. The DA transport V_{max} (mol × 10^{-16}/cell/min) and K_m (in micromoles) values, respectively, were as follows: hNET, 1.0 ± 0.2 and 1.5 ± 0.7; R121Q, 1.0 ± 0.3 and 1.9 ± 0.9; N292T, 0.5 ± 0.1 and 1.1 ± 0.5; F528C, 1.2 ± 0.2 and 1.4 ± 0.5; and Y548H, 0.9 ± 0.2 and 1.4 ± 0.6.

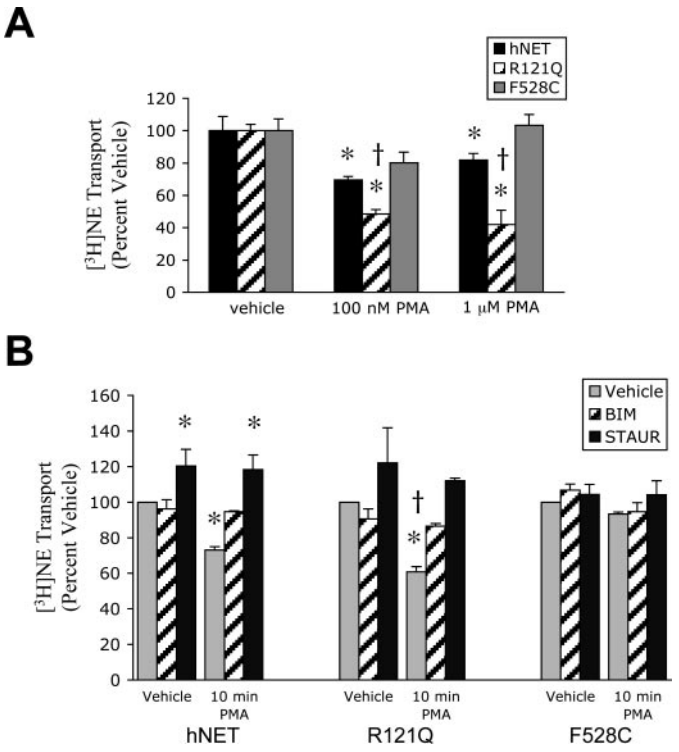

Fig. 6. Effects of β-PMA treatment on [^{3}H]NE transport by hNET and variants. COS-7 cells were transfected with hNET or variant cDNAs. Twenty-four hours later, β-PMA and PKC-inhibitor treatments were performed as described under *Materials and Methods*. A, COS-7 cells transfected with hNET (■), R121Q (▨) or F528C (▤) cDNAs were incubated in 100 nM or 1 μM β-PMA for 30 min followed by 10-min uptake of 50 nM [^{3}H]NE. [^{3}H]NE transport for vehicle-treated groups were 2.0 ± 0.2, 1.6 ± 0.1, and 4.9 ± 0.4 mol × 10^{-18}/cell/min for hNET, R121Q and F528C, respectively. Data are mean ± S.E.M., $n = 3$. Data were analyzed by one-way ANOVA, *, $p < 0.0.05$ compared with vehicle for that variant; †, $p < 0.05$ compared with PMA-treated hNET. B, COS-7 cells transfected with hNET or variant cDNAs were incubated in vehicle (▤), 1 μM BIM (▨), or 1 μM staurosporine (■) for 20 min before the addition of 100 nM β-PMA for 10 min followed by 10-min uptake of 50 nM [^{3}H]NE. [^{3}H]NE transport for vehicle-vehicle groups were 5.2 ± 1.4, 3.1 ± 0.9, and 7.0 ± 1.6 mol × 10^{-18}/cell/min for hNET, R121Q, and F528C, respectively. Data are expressed as the percentage of vehicle-vehicle–treated hNET or variant and are the mean ± S.E.M. of three experiments. Data were analyzed by one-way ANOVA for each variant; *, $p < 0.0.05$ compared with vehicle-vehicle group within hNET or variant; †, $p < 0.05$ compared with hNET vehicle/PMA group.

of negative selection pressure, as evidenced by the positive BLOSUM62 scores of this group and the presence of alternate amino acids at several of these positions in NET of other species (Table 2). Other amino acid substitutions at these positions, however, have revealed some functional impact. Whereas the extracellular loop 4 variant N375S was without effect, N375P increases uptake 2-fold (Roubert et al., 2001). Likewise, the engineered mutant V356S demonstrates an increase in DA uptake and a decreased affinity for nortriptyline and desipramine, whereas the naturally occurring polymorphism V356L did not differ in transport or antagonist affinity.

More than half of the SNPs examined resulted in demonstrable changes in expression, activity, binding, or regulation, and, moreover, these SNPs correlated with negative BLOSUM62 scores, indicating unfavorable substitutions. A369P generated the most dramatic effect, revealing a complete lack of transport of NE and DA that was accompanied by a total loss of the surface 110-kDa protein. The 54-kDa form of A369P was expressed on the surface, yet this species was nonfunctional. Because we detected minimal accumulation of the immature form of A369P and a form migrating at a molecular mass higher than the 110-kDa form that we suspect represents intracellular aggregates, A369P is likely to be a misfolded protein that is targeted for degradation after exit from the endoplasmic reticulum, a pattern similar to that observed for the hNET A457P mutation (Hahn et al., 2003). An hNET mutant of multiple residues that incorporates amino acids close to Ala369 in extracellular loop 4 also does not transport (Roubert et al., 2001), pointing to an important role for extracellular loop 4 in transporter biosynthesis and function.

Two of the mutants, Y548H and N292T, displayed a graded loss of both DA and NE transport. Transport deficits of N292T were similar in degree to reductions in levels of the 110-kDa form, indicating that the 54-kDa form, which demonstrated increased surface expression, is not functional. It is interesting to note that a triple mutation in the third extracellular loop that includes an N292R substitution exhibited a 7-fold increased capacity for DA transport (Roubert et al., 2001). Y548H, located in extracellular loop 6, reduced both NE and DA uptake and surface transporter by approximately 20%. I549T also demonstrated a decrease in protein but not in transport. The disparity between these measures for I549T remains to be clarified in future studies, but its proximity to Tyr548 suggests a sensitivity of this region of the transporter to substitutions.

The variants discussed thus far that affected transport, A369P, N292T, and Y548H, are located in extracellular loops 3 to 6, and these loops, as well as proximal TMs, have been implicated in transport function. Studies of DAT/NET chimeras suggest that the region spanning TMs 4 to 9 are critical for substrate translocation (Buck and Amara, 1994). Chimeras of SERT containing the NET extracellular loops 4, 5, or 6 retain antagonist selectivity but demonstrate greatly reduced transport activity (Smicun et al., 1999). Furthermore, methanethiosulfonate reagent sensitivity studies reveal that residues close to the extracellular face of TM 7 or 8 of human DAT are important for substrate and antagonist interactions (Norregaard et al., 2003).

F528C, located in TM 11, demonstrated a selective change in transport of NE versus DA, which is evident from an increase in both the ratio of NE to DA transport and from the ratio of V_{max} to K_m for NE compared with hNET. F528C does

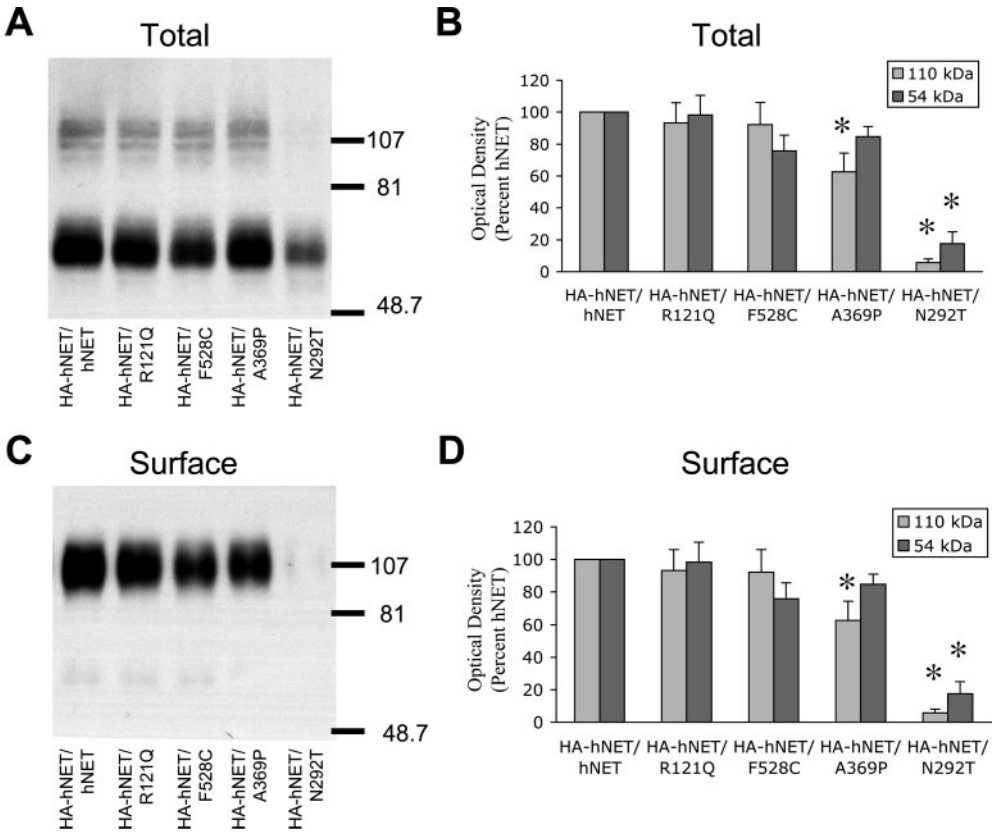

Fig. 7. Effects of cotransfection of hNET variants on hNET expression. COS-7 cells were transfected with HA-tagged hNET or variant hNET cDNAs and experiments were performed 24 h later. Biotinylation and Western blot analyses were performed as described under *Materials and Methods*. Total cellular lysate (A) and surface (C) proteins were blotted with an HRP-conjugated anti-HA antibody. Molecular mass standards are indicated in kilodaltons. Quantification of hNET and variant protein expression in total (B) and surface fractions (D) was performed by determining optical density measurements for each band with ImageJ software as described under *Materials and Methods*. Results are expressed as the percentage of hNET band density for each protein species and are the mean ± S.E.M. from three experiments. Data were analyzed by one-way ANOVA as described under *Materials and Methods;* *, $p < 0.05$ compared with hNET of corresponding molecular mass form.

not differ from hNET in K_i values for NE competition of either [^{3}H]nisoxetine binding or [^{3}H]DA uptake, suggesting that there is an increase in translocation efficiency of NE at F528C (data not shown). Residues in TM 11 and 12 of SERT influence potencies of both substrates and tricyclic antidepressants (Barker et al., 1994). Similar to F528C, S545A in TM 11 of SERT, corresponding to Ser525 in hNET, increases the V_{max} for serotonin transport and decreases the binding affinity for the tricyclic antidepressant imipramine (Sur et al., 1997). Furthermore, a single phenylalanine in this region directs the potency of hSERT for tricyclic antidepressants (Barker and Blakely, 1996). In contrast, F530A in rat DAT, corresponding to Phe528 in hNET, demonstrates little effect on expression levels, yet transport activity is reduced by more than 90% (Lin et al., 1999). To the extent that F528C may be enriched in an extreme blood pressure phenotype, it could influence tricyclic treatment response in such individuals. Taken together, our data and the results of mutational analyses support the involvement of TM 11 generally, and F528 in hNET specifically in both substrate affinities and translocation and antagonist affinities.

The phenotype of R121Q highlights the important role of intracellular loop 1 in transporter trafficking and regulation. The greater impact on NE transport, compared with either DA transport or surface protein levels, is inconsistent with an impact conferred solely by altered surface density. Sucic and Bryan-Lluka (2002) noted that Arg121 is part of the conserved sequence GXXXRXG that is similar to a GXXXXRXG motif present in the bacterial Tn10 tetracycline antiporter and in which the positively charged arginine is required for transport (Yamaguchi et al., 1992). These authors also observed reductions in transport and expression with substitution of glycine at Arg121 in NET (Sucic and Bryan-Lluka, 2002). It is interesting to note that conversion of rat DAT intracellular loop 1 to the corresponding hNET residues decreases basal uptake and blocks ethanol-induced activation of rat DAT (Maiya et al., 2002). Our preliminary studies indicate that R121Q also is more sensitive to the effects of ethanol (data not shown).

The ability of variants R121Q and F528C to selectively confer changes to NE versus DA transport has precedent in other studies of mutations that produce a substrate-selective impact on transport. For example, species differences between *Drosophila melanogaster* and human SERTs in binding and transport affinities for substituted tryptamines, but not serotonin, can be closely recapitulated by the single mutation Y95F in human SERT (Adkins et al., 2001). Studies of rat and human SERT chimeras indicate that TMs 11 and 12 of human SERT account for the difference in the potency of D-amphetamine relative to rat SERT, whereas serotonin recognition is unaffected (Barker et al., 1994). Differences in substrate usage by hNET variants suggest a potential impact of variants on the balance of catecholamine neurotransmission in areas of the central nervous system in which dual innervation by NE and DA occurs. In the prefrontal cortex, in which both NE and DA fibers are present, released DA is cleared from the extracellular space by NET (Gresch et al., 1995). The therapeutic effect of selective NET blockers in the treatment of ADHD may lie in their ability to elevate both NE and DA.

The observation that F528C was insensitive and R121Q more sensitive to β-PMA suggests that similar mechanisms may underlie differences observed in both basal and regulated transport. F528C was insensitive to staurosporine inhibition, supporting that PKC activity present in untreated cells may play a part in differences we observe in basal transport. In addition, PKC-induced down-regulation results not only in a decrease in hNET V_{max} but also influences NET intrinsic activity (Apparsundaram et al., 1998; Sung et al., 2003), and such a function may play a role in effects observed on hNET variants in the present study.

A369P and N292T both decreased total and surface levels of hNET, supporting growing evidence that intracellularly retained or mistargeted variants exert dominant-negative effects to decrease surface expression and activity of wild-type transporters facilitated by the formation of oligomeric complexes (Hahn et al., 2003; Sitte et al., 2004). Elevated levels of unglycosylated and anomolously glycosylated N292T may additionally saturate synthesis and glycosylation processes. N292T accumulates in lower mass forms while greatly diminishing cotransfected hNET, which suggests that N292T may be a more stable protein. The normal core glycosylation but defect in late-stage glycosylation exhibited by A369P is similar to that of our previously described variant A457P, a variant that restricts hNET surface expression and has a dominant-negative impact on hNET transport (Hahn et al., 2003). It was somewhat surprising that neither N292T nor A369P diminished transport to an extent that might be predicted from the effect on hNET protein. A457P exhibits measurable surface expression of a nonfunctional 110-kDa form that may contribute to its dominant-negative influence on transport. In addition, the lack of effect on transport may reflect a limitation of heterologous expression in which overexpression and unknown stoichiometry of interacting proteins may mask effects. Cotransfection of hNET with F528C or R121Q yielded shifts in the β-PMA response that were intermediate to the effects on either hNET or variant alone. Thus, one regulation phenotype did not dominate function under conditions of coexpression. Taken together, these results, coupled with our previous data and those of other groups, support that dominant-negative associations with variants can occur at early stages of transporter biosynthesis to influence hNET biosynthetic progression, whereas evidence of functional interactions between subunits at the level of the plasma membrane remain to be explored further.

The present data reveal striking influences of naturally occurring *hNET* coding variants on hNET function that may indeed contribute to in vivo function, as suggested by their discovery in cardiovascular phenotypes. In this regard, a recently identified SERT variant demonstrates both faster translocation and altered response to second messengers in vitro and can be tracked in carriers within two families presenting with complex psychiatric profiles, including obsessive-compulsive disorder and social phobia (Kilic et al., 2003). It will be important to examine the expression of hNET variants in transfected neuronal culture, in which depolarization, second messengers, and voltage-sensitive transporter-associated currents probably all play a role in regulating transporter activity (Galli et al., 1998; Savchenko et al., 2003). In addition, genetically modified mice bearing functional variants should facilitate the analysis of systems-level questions of transporter response in the face of neuronal excitability and second-messenger activation, the influence

of substrate selectivity, and the impact of these factors on behavior.

Acknowledgments

We thank Angela Steele for construction of the V244I and I549T plasmids and Dr. Uhna Sung and Jane Wright for construction of the HA-hNET plasmid. We gratefully acknowledge Tammy Jessen for general laboratory management, Qiao Han for oversight of cell culture facilities, and the Neurogenomics Core of the Center for Molecular Neuroscience (Vanderbilt University Medical Center).

References

Adkins EM, Barker EL, and Blakely RD (2001) Interactions of tryptamine derivatives with serotonin transporter species variants implicate transmembrane domain I in substrate recognition. *Mol Pharmacol* **59:**514–523.

Apparsundaram S, Schroeter S, Giovanetti E, and Blakely RD (1998) Acute regulation of norepinephrine transport: II. PKC-modulated surface expression of human norepinephrine transporter proteins. *J Pharmacol Exp Ther* **287:**744–751.

Barker EL and Blakely RD (1996) Identification of a single amino acid, phenylalanine 586, that is responsible for high affinity interactions of tricyclic antidepressants with the human serotonin transporter. *Mol Pharmacol* **50:**957–965.

Barker EL, Kimmel HL, and Blakely RD (1994) Chimeric human and rat serotonin transporters reveal domains involved in recognition of transporter ligands. *Mol Pharmacol* **46:**799–807.

Biederman J and Spencer T (1999) Attention-deficit/hyperactivity disorder (ADHD) as a noradrenergic disorder. *Biol Psychiatry* **46:**1234–1242.

Blakely RD (2001) Physiological genomics of antidepressant targets: keeping the periphery in mind. *J Neurosci* **21:**8319–8323.

Buck KJ and Amara SG (1994) Chimeric dopamine-norepinephrine transporters delineate structural domains influencing selectivity for catecholamines and 1-methyl-4- phenylpyridinium. *Proc Natl Acad Sci USA* **91:**12584–12588.

Fuller RW and Hemrick-Luecke SK (1983) Antagonism by tomoxetine of the depletion of norepinephrine and epinephrine in rat brain by alpha-methyl-m-tyrosine. *Res Commun Chem Pathol Pharmacol* **41:**169–172.

Galli A, Blakely RD, and DeFelice LJ (1998) Patch-clamp and amperometric recordings from norepinephrine transporters: channel activity and voltage-dependent uptake. *Proc Natl Acad Sci USA* **95:**13260–13265.

Gresch PJ, Sved AF, Zigmond MJ, and Finlay JM (1995) Local influence of endogenous norepinephrine on extracellular dopamine in rat medial prefrontal cortex. *J Neurochem* **65:**111–116.

Hahn MK and Blakely RD (2002a) Gene organization and polymorphisms of monoamine transporters. Relationship to psychiatric and other complex diseases, in *Neurotransmitter Transporters. Structure*, *Function and Regulation* (Reith MEA, ed) pp 111–169, Humana Press, Totowa.

Hahn MK and Blakely RD (2002b) Monoamine transporter gene structure and polymorphisms in relation to psychiatric and other complex disorders. *Pharmacogenomics* **2:**217–235.

Hahn MK, Robertson D, and Blakely RD (2003) A mutation in the human norepinephrine transporter gene (SLC6A2) associated with orthostatic intolerance disrupts surface expression of mutant and wild-type transporters. *J Neurosci* **23:**4470–4478.

Halushka MK, Fan JB, Bentley K, Hsie L, Shen N, Weder A, Cooper R, Lipshutz R, and Chakravarti A (1999) Patterns of single-nucleotide polymorphisms in candidate genes for blood-pressure homeostasis. *Nat Genet* **22:**239–247.

Heim C and Nemeroff CB (2001) The role of childhood trauma in the neurobiology of mood and anxiety disorders: preclinical and clinical studies. *Biol Psychiatry* **49:**1023–1039.

Henikoff S and Henikoff JG (1992) Amino acid substitution matrices from protein blocks. *Proc Natl Acad Sci USA* **89:**10915–10919.

Iversen LL (1961) The uptake of noradrenaline by the isolated rat heart. *Br J Pharmacol* **21:**523–537.

Iwasa H, Kurabayashi M, Nagai R, Nakamura Y, and Tanaka T (2001) Genetic variations in five genes involved in the excitement of cardiomyocytes. *J Hum Genet* **46:**549–552.

Keller NR, Diedrich A, Appalsamy M, Tuntrakool S, Lonce S, Finney C, Caron MG, and Robertson D (2004) Norepinephrine transporter-deficient mice exhibit excessive tachycardia and elevated blood pressure with wakefulness and activity. *Circulation* **110:**1191–1196.

Kilic F, Murphy DL, and Rudnick G (2003) A human serotonin transporter mutation causes constitutive activation of transport activity. *Mol Pharmacol* **64:**440–446.

Klimek V, Stockmeier C, Overholser J, Meltzer HY, Kalka S, Dilley G, and Ordway GA (1997) Reduced levels of norepinephrine transporters in the locus coeruleus in major depression. *J Neurosci* **17:**8451–8458.

Leabman MK, Huang CC, DeYoung J, Carlson EJ, Taylor TR, de la Cruz M, Johns SJ, Stryke D, Kawamoto M, Urban TJ, et al. (2003) Natural variation in human membrane transporter genes reveals evolutionary and functional constraints. *Proc Natl Acad Sci USA* **100:**5896–5901.

Lin Z, Wang W, Kopajtic T, Revay RS, and Uhl GR (1999) Dopamine transporter: transmembrane phenylalanine mutations can selectively influence dopamine uptake and cocaine analog recognition. *Mol Pharmacol* **56:**434–447.

Maiya R, Buck KJ, Harris RA, and Mayfield RD (2002) Ethanol-sensitive sites on the human dopamine transporter. *J Biol Chem* **277:**30724–30729.

Melikian HE, McDonald JK, Gu H, Rudnick G, Moore KR, and Blakely RD (1994) Human norepinephrine transporter. Biosynthetic studies using a site-directed polyclonal antibody. *J Biol Chem* **269:**12290–12297.

Melikian HE, Ramamoorthy S, Tate CG, and Blakely RD (1996) Inability to *N*-glycosylate the human norepinephrine transporter reduces protein stability, surface trafficking and transport activity but not ligand recognition. *Mol Pharmacol* **50:**266–276.

Norregaard L, Loland CJ, and Gether U (2003) Evidence for distinct sodium-, dopamine- and cocaine-dependent conformational changes in transmembrane segments 7 and 8 of the dopamine transporter. *J Biol Chem* **278:**30587–30596.

Pacholczyk T, Blakely RD, and Amara SG (1991) Expression cloning of a cocaine- and antidepressant-sensitive human noradrenaline transporter. *Nature (Lond)* **350:**350–354.

Ressler KJ and Nemeroff CB (1999) Role of norepinephrine in the pathophysiology and treatment of mood disorders. *Biol Psychiatry* **46:**1219–1233.

Roubert C, Cox PJ, Bruss M, Hamon M, Bonisch H, and Giros B (2001) Determination of residues in the norepinephrine transporter that are critical for tricyclic antidepressant affinity. *J Biol Chem* **276:**8254–8260.

Runkel F, Bruss M, Nothen MM, Stober G, Propping P, and Bonisch H (2000) Pharmacological properties of naturally occurring variants of the human norepinephrine transporter. *Pharmacogenetics* **10:**397–405.

Savchenko V, Sung U, and Blakely RD (2003) Cell surface trafficking of the antidepressant-sensitive norepinephrine transporter revealed with an ectodomain antibody. *Mol Cell Neurosci* **24:**1131–1150.

Schomig E, Fischer P, Schonfeld CL, and Trendelenburg U (1989) The extent of neuronal re-uptake of ^{3}H-noradrenaline in isolated vasa deferentia and atria of the rat. *Naunyn-Schmiedeberg's Arch Pharmacol* **340:**502–508.

Shannon JR, Flattem NL, Jordan J, Jacob G, Black BK, Biaggioni I, Blakely RD, and Robertson D (2000) Clues to the origin of orthostatic intolerance: a genetic defect in the cocaine- and antidepressant sensitive norepinephrine transporter. *N Eng J Med* **342:**541–549.

Sitte HH, Farhan H, and Javitch JA (2004) Sodium-dependent neurotransmitter transporters: oligomerization as a determinant of transporter function and trafficking. *Mol Interv* **4:**38–47.

Smicun Y, Campbell SD, Chen MA, Gu H, and Rudnick G (1999) The role of external loop regions in serotonin transport. Loop scanning mutagenesis of the serotonin transporter external domain. *J Biol Chem* **274:**36058–36064.

Stöber G, Nothen MM, Porzgen P, Bruss M, Bonisch H, Knapp M, Beckmann H, and Propping P (1996) Systematic search for variation in the human norepinephrine transporter gene: identification of five naturally occurring missense mutations and study of association with major psychiatric disorders. *Am J Med Genet* **67:**523–532.

Sucic S and Bryan-Lluka LJ (2002) The role of the conserved GXXXRXG motif in the expression and function of the human norepinephrine transporter. *Brain Res Mol Brain Res* **108:**40–50.

Sung U, Apparsundaram S, Galli A, Kahlig K, Savchenko V, Schroeter S, Quick MW, and Blakely RD (2003) A regulated interaction of syntaxin 1A with the antidepressant-sensitive norepinephrine transporter establishes catecholamine clearance capacity. *J Neurosci* **23:**1697–1709.

Sur C, Betz H, and Schloss P (1997) A single serine residue controls the cation dependence of substrate transport by the rat serotonin transporter. *Proc Natl Acad Sci USA* **94:**7639–7644.

Tatsumi M, Groshan K, Blakely RD, and Richelson E (1997) Pharmacological profile of antidepressants and related compounds at human monoamine transporters. *Eur J Pharmacol* **340:**249–258.

Xu F, Gainetdinov RR, Wetsel WC, Jones SR, Bohn LM, Miller GW, Wang YM, and Caron MG (2000) Mice lacking the norepinephrine transporter are supersensitive to psychostimulants. *Nat Neurosci* **3:**465–471.

Yamaguchi A, Someya Y, and Sawai T (1992) Metal-tetracycline/H+ antiporter of Escherichia coli encoded by transposon Tn10. The role of a conserved sequence motif, GXXXXRXGRR, in a putative cytoplasmic loop between helices 2 and 3. *J Biol Chem* **267:**19155–19162.

Address correspondence to: Dr. Randy D. Blakely, Center for Molecular Neuroscience, 6133 Medical Research Building III, Suite 7140, Vanderbilt School of Medicine, Nashville, TN 37232-8548. E-mail: randy.blakely@vanderbilt.edu